25th ABCM International Congress of Mechanical Engineering
October 20-25, 2019, Uberlândia, MG, Brazil

COB-2019- 0078
STABILITY OF A FLEXIBLE ROTOR WITH LUBRICATED BEARINGS – A STOCHASTIC APPROACH

Laís Bittencourt Visnadi
Helio Fiori de Castro
University of Campinas
lais.visnadi@fem.unicamp.br, heliofc@fem.unicamp.br

Abstract. *This paper considers the impact of variabilities of bearing parameters on the threshold of stability of rotating systems, considering the fluid-induced instability. A Laval model of rotor was considered supported by cylindrical hydrodynamic bearings. The parameters considered to present variabilities were the bearing clearance and the oil viscosity. It was indicated that the uncertainties around the stability threshold depend on the position of the shaft on the bearing and the stability limit for the system. These aspects are characterized by two curves, and the region that they cross each other are determinant for the uncertainties presented on the stability threshold. This analysis was done applying additional static loads on the shaft.*

Keywords: *Rotating machinery, Laval model, Fluid-induced stability, Stability threshold, Uncertainty quantification.*

1. INTRODUCTION

Rotating machinery are present in many industrial sectors, such as mechanical, chemical and energy generation. These machines, when supported by hydrodynamic bearings (mainly cylindrical), are subjected to fluid-induced instability, a condition that can cause severe damage to the machine parts. This instability is related to the shaft rotation speed (Newkirk, 1925) and it is possible to define a maximum allowed rotating speed for a safe operation, so that the unstable operation is avoided. However, the parameters that define this threshold are subjected to variabilities, due to measurement uncertainties, errors or even operational temperature variations, which may cause variations on system response.

Laval, in 1895, proposed a rotor model considering a long and flexible shaft with negligible mass, bi-supported by a rigid structure, with a centered disc. This model is simple, but is useful for understanding rotor phenomena and it is the model applied on this paper. The bearings are modeled by the Reynolds Equation (Reynolds, 1886), which is applied by considering the bearing clearance as small. Ocvirk (1952) obtained an analytical solution for Reynolds Equation by considering a short bearing, so the pressure gradient on the circumferential direction could be neglected.

Product variabilities will always occur, since it's not possible to control all the parameters that influence on its characteristics. Even when there is a control, it is susceptible to errors or imprecision. Although many engineering problems are solved with deterministic models, not considering this possible variabilities may generate different results than the expected when the product is produced and put into operation.

The Monte Carlo Method is used in this study for solving the stochastic problem. The parameter variabilities may be modeled by probability density functions, which may be obtained by histograms generated from experiments or by applying the Maximum Entropy Principle, which considers the known information about the variable (Shannon, 1948). After generating input samples according to the designated distribution, the deterministic model is solved for each sample item, and finally the results are analyzed statistically.

This study is a continuation of a previous study (Visnadi and Castro, 2018), in which the variability of the stability threshold was investigated considering variabilities on the bearing length, radius, radial clearance and oil viscosity for Laval rotors with different disc masses. The present paper analyses the variability of the stability threshold considering variabilities on the radial bearing clearance and the oil viscosity, since they are the parameters that present more variabilities on real situations. In addition, the influence of different static loads on the bearings, instead of disc masses (that change the natural frequency of the system) on the uncertainties around the stability threshold is investigated.

2. SYSTEM MODELING

The Laval model consists on a flexible shaft, with circular transverse area and negligible mass. A centered disc, perpendicular to the longitudinal direction of the shaft, may or may not have its center of gravity coincident to its centroid. It is possible to consider that this shaft is supported by hydrodynamic bearings (Krämer, 1993), although the original proposal was to consider a support with rigid bearings.

Figure 1 shows the two coordinate systems applied on the rotor, which are necessary to define its equations of motion, since the deflection of the shaft makes the disc center not to coincide with the journal center inside the bearings. The static distance between the journal center and the centroid of the disc is indicated as y_s. The journal eccentricity (e_j) is the distance of the bearing center to the journal center. The disc eccentricity (e) is the distance between the centroid of the disc and its center of gravity, which will be considered negligible in this study. The shaft rotational speed is Ω.

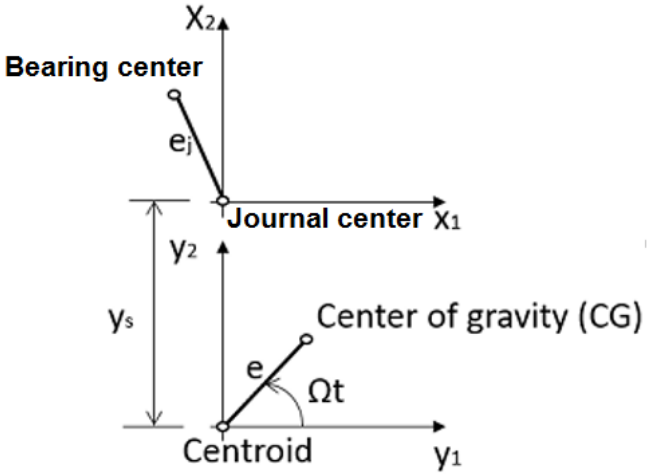

Figure 1. Coordinate system adopted for a Laval Rotor with hydrodynamic bearings (Krämer, 1993).

It is possible to define the equations of motion for this system, considering the disc mass (m) and the stiffness coefficient of the shaft (k):

$$m\ddot{y}_1 + k(y_1 - x_1) = 0 \tag{1}$$

$$m\ddot{y}_2 + k(y_2 - x_2) = 0 \tag{2}$$

The static displacement y_s is calculated considering the disc weight and the shaft flexibility:

$$y_s = \frac{mg}{k} \tag{3}$$

Figure 2 shows the cylindrical hydrodynamic bearing considered in this study. It is defined that its length is , its radius is R, and its clearance is h_o. The shaft radius is defined as r.

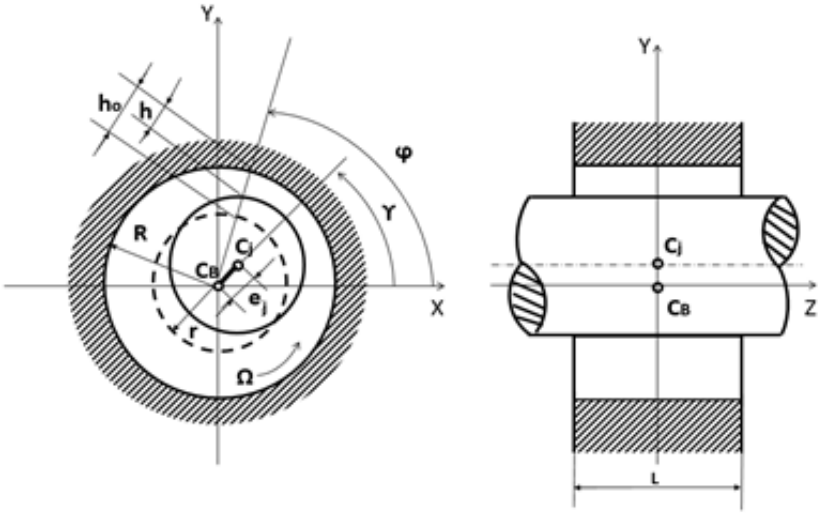

Figure 2. Scheme of hydrodynamic bearing (Krämer, 1993).

It is assumed that Reynolds Equation is valid for describing the oil film condition. The relation $L/2R \leq 0.5$ is applied and pressure variations on the circumferential direction are negligible compared to pressure variations on axial direction ($\partial p/\partial \varphi = 0$) (Ocvirk 1952). The pressure function may be obtained from Reynolds Equation, applying $dp/dz = 0$ for $z = 0$ and $p = 0$ for $z = \pm L/2$:

$$p(\varphi, z, t) = \frac{3\eta}{h^3}\left[e_j(\Omega - 2\dot{\gamma})\sin(\varphi - \gamma) - 2\dot{e}_j\cos(\varphi - \gamma)\right]\left(z^2 - \frac{L^2}{4}\right) \tag{4}$$

By integrating Eq. (4) on Z, it is possible to obtain the oil-film force by length unit on circumferential direction. By integrating on the circumferential direction and adapting to the proper coordinate system, it is possible to obtain the vertical and horizontal forces on the shaft, F_1 and F_2, respectively.

By partially differentiating the forces $F_1$and F_2 by x_1 and x_2, the bearing stiffness and damping coefficients are obtained (Krämer, 1993):

$$\frac{\partial F_i}{\partial x_k} = k_{ik} \tag{5}$$

$$\frac{\partial F_i}{\partial \dot{x}_k} = d_{ik} \tag{6}$$

i=1,2 and k=1,2.

Equations of motion considering linear forces on the shaft are:

$$k(x_1 - y_1) + 2(k_{11}x_1 + k_{12}x_2) + 2(d_{11}\dot{x}_1 + d_{12}\dot{x}_2) = 0 \tag{7}$$

$$k(x_2 - y_2) + 2(k_{21}x_1 + k_{22}x_2) + 2(d_{21}\dot{x}_1 + d_{22}\dot{x}_2) = 0 \tag{8}$$

Equations (7) and (8), associated with Eq. (1) and (2) provide the displacements of the journal center and the displacements of the disc centroid.

The eigenvalues of the equations of motion are complex conjugate. The system is stable if the real part is negative, but if it is positive, the system is unstable, since vibration is increasing along time. It is considered that, if the real part is equal to zero, it means that the system is to become unstable, so it is at the stability threshold. Considering it, a equation for the stability threshold as a function of the shaft rotational speed and associated to the eccentricity ratio of the shaft $\left(\varepsilon = \frac{e_j}{h_o}\right)$ is determined. It is called the borderline curve (Krämer, 1993).

The shaft eccentricity ratio (ε) describes the position of the shaft inside the bearing. For a horizontally supported rotor ($F_1 = 0$ and $F_2 = mg$), the shaft is next to bearing surface in the beginning of operation, so that the eccentricity ratio is equal to one. As the shaft rotational speed increases, the shaft tends to align with the bearing center. This movement is described by Eq. (9), called startup curve (Krämer, 1993). It is noteworthy that it is related to the bearing static load ($F_o = \frac{F_2}{2} + F_{ad}$ for a symmetrical rotor. $F_{ad}$is a possible additional static load on the bearing, not related to the disk mass) and to the shaft friction force (F_η) described by Eq. (10).

$$\frac{F_o}{F_\eta} = \frac{\pi}{2}\frac{\varepsilon}{(1-\varepsilon^2)^2}\sqrt{1 - \varepsilon^2 + \left(\frac{\pi}{4}\varepsilon\right)^2} \tag{9}$$

In which the shaft friction force (F_η) is given by:

$$F_\eta = \frac{\eta L^3 \Omega R}{2h_o^2} \tag{10}$$

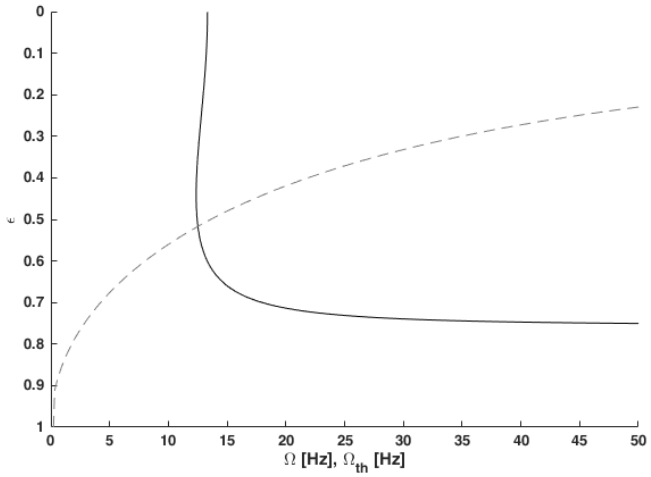

Figure 3. Startup curves (dashed) and stability borderline (solid) for a hypothetical system

Figure 3 shows an example of startup curve (dashed line) and borderline curve (solid line) for a system. The rotational speed in which the startup curve crosses the borderline curve is the stability threshold: for higher rotational speeds, the system is unstable.

3. STOCHASTIC MODELING

As it is intended to analyze the threshold of stability considering uncertainties on bearing parameters, it is necessary to model these parameters as probability density functions instead of deterministic values. Since there is experimental data about these parameters it was considered that the information known about the parameters were the support interval (between 0 and ∞), the mean and the standard deviation. Because of that, the distribution that chosen to describe the parameters uncertainties is Gamma distribution (G):

$$G(\alpha,\beta) = f(y) = \begin{cases} \frac{1}{\Gamma(\alpha)\beta^{\alpha}} y^{\alpha-1} e^{-y/\beta}, & 0 < y < \infty \\ 0, & y \leq 0 \end{cases} \tag{11}$$

This distribution is characterized by a shape parameter (α) and a scale parameter (β), which can be related to the mean value and the standard deviation of the distribution by Eq. (12) and (13) (Montgomery and Runger, 2014):

$$\mu = \alpha.\beta \tag{12}$$

$$\sigma = \sqrt{\alpha.\beta^2} \tag{13}$$

The Monte Carlo Method consists on solving the deterministic model for a sample of input parameters. Then, the system response is not a single value, but also a distribution. To generate the parameters samples, a random number generator based on the algorithms proposed by Devroye (1986) was used.

4. RESULTS

In this paper, the influences of variabilities on bearing clearance (h_o) and the oil viscosity (η) on the stability threshold were analyzed for a Laval rotor. Table 1 presents the value of each rotor and bearing parameter considered for the convergence analysis of the Monte Carlo Method. The values of on bearing clearance (h_o) and the oil viscosity (η) presented on Tab. 1 are their mean values, and their variance was 5% of their respective mean value.

Table 1. System parameters values considered for the convergence analysis of the Monte Carlo Method

Disc mass (m) [kg]	8.0
Shaft diameter (D_s) [m]	0.012
Shaft length (L_s) [m]	0.600
Shaft elasticity model (E) [Pa]	210x109
Radial bearing clearance h_0 [μm]	90
Oil viscosity η [Pa.s]	0.04
Bearing length L [m]	0.02

Bearing radius R [m]	0.015

Figure 4 shows the normalized histogram (for probability) for generated samples of 3,000 numbers, 5,000 numbers and 10,000 numbers. It is possible to notice that there is some difference between the 3,000 numbers histogram and the 5,000 numbers histogram. The differences between the 5,000 numbers histogram and the 10,000 numbers histogram are minimum. Table 2 presents the mean value and the standard deviations. It shows that mean values and standard deviations are nearly the same for all samples sizes. Therefore, by comparing the histograms, it was considered that the Monte Carlo Method convergence was obtained with a 5,000 objects sample.

Figures 5, 6 and 7 show the startup curves (gray) and the borderline curves (black) for rotors with different disc masses (2.5 kg, 8 kg and 35kg, respectively). They also present a histogram of the stability threshold (light gray bars). Table 3 details the maximum safe shaft rotational speed, the mean value, the standard deviation, the skewness and kurtosis of the histograms and the instability zones.

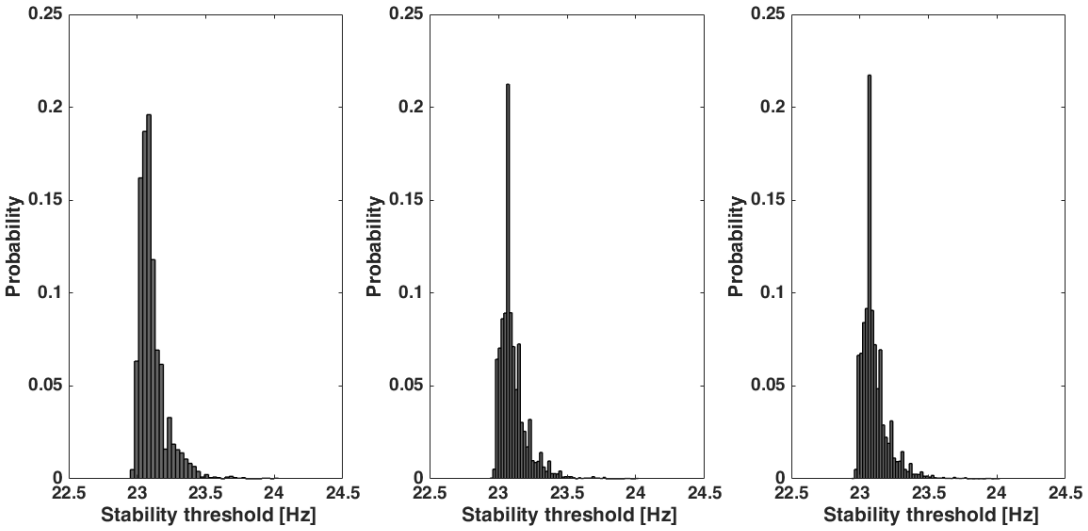

Figure 4. Normalized histogram for the stability threshold for samples with 3,000, 5,000 and 10,000 generated numbers, respectively.

Table 2. Mean and standard deviations of the data of the transition of stability for 3,000, 5,000 and 10,000 objects samples.

Objects in sample	Mean [Hz]	Standard Deviation [Hz]
3,000	23.11	0.11
5,000	23.10	0.10
10,000	23.10	0.10

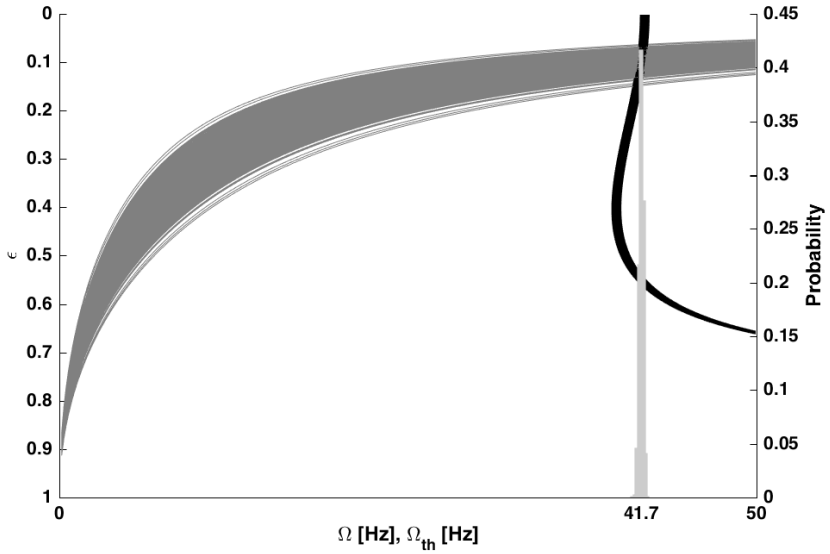

Figure 5. Startup curves (gray), borderline curves (black) and histogram of the stability threshold (light gray vertical bars) for the considered system with an 2.5kg disc mass

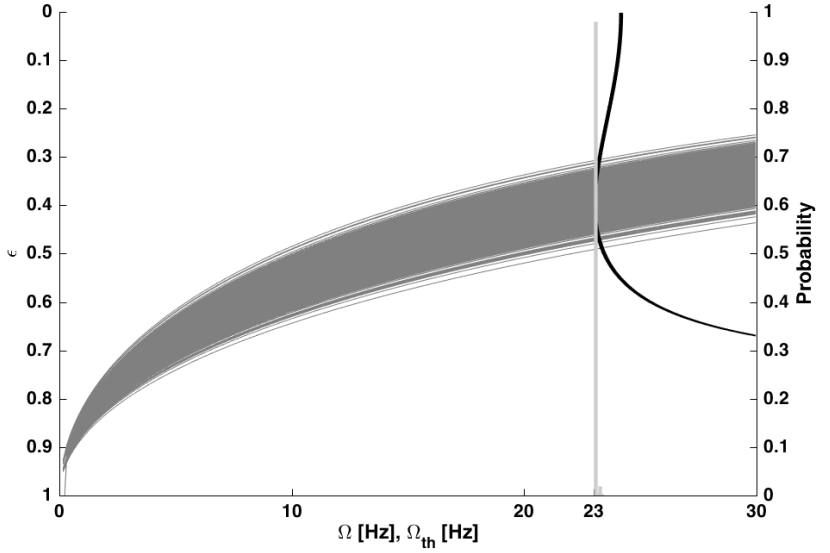

Figure 6. Startup curves (gray), borderline curves (black) and histogram of the stability threshold (light gray vertical bars) for the considered system with an 8kg disc mass

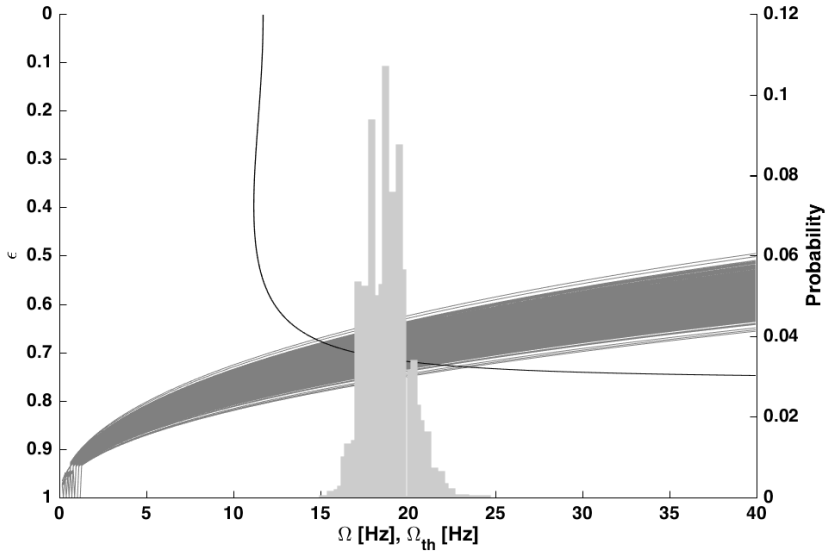

Figure 7. Startup curves (gray), borderline curves (black) and histogram of the stability threshold (light gray vertical bars) for the considered system with an 35kg disc mass

Table 3. Summary of the results for the simulated systems

Disc mass [kg]	Natural frequency [Hz]	Maximum safe rotational speed [Hz]	Mean [Hz]	Standard deviation [Hz]	Skewness	Kurtosis	Instability zone [Hz]
2.5	21.94	41.06	41.71	0.15	0.21	3.07	41.06-42.18
8	12.26	23.08	23.08	0.02	7.19	54.72	23.08 - 23.40
35	5.86	15.12	18.69	1.18	0.39	3.24	15.12-24.51

Figure 5 shows that, for a considered "light" rotor (2.5 kg), the shaft tends to get to the bearing center as its rotational speed increases. Figures 6 and 7 show that, for higher disc masses, the shaft doesn't get to the center. The natural frequency of the system has an influence on the borderline curve: for a higher mass, the natural frequency decreases and the borderline curve moves to the left. The threshold of stability is the point that the startup curve crosses the borderline curve. This crossing occurs at a higher rotational speed for lower masses and at a lower rotational speed for higher disc masses. Table 3 shows the detailed data of the presented histograms. The results agree with the previous study of Visnadi and Castro (2018).

The same previous study (Visnadi and Castro, 2018) highlighted that the 35kg disc mass was a hypothetical situation to observe a high variability on the stability threshold, since this system has a low natural frequency.

The same effect of modifying the curves crossing region may be obtained by adding a static force on the bearing. This may occur on real systems if the disc is a loaded gear, for example. The difference of this case is that it does not change the natural frequency of the system, so that the borderline curve does not displace to the left, as it occurs when the mass is increased.

This situation for the system with a 2.5kg disc with an additional load of 80 N in each bearing, with oil viscosity and bearing clearance presenting the variabilities same on previous cases is shown in Fig. 8. It is possible to notice that this system presents low variabilities on the stability threshold because of the region of crossing curves, but it was maintained at around 40 Hz.

Figure 9 shows the same system, but only the additional load presents variability, with standard deviation of 5% of its mean value. It was also modeled as a gamma distribution because the possibility of negative force (which would be an upright force on the bearing) was neglected. The variability of the additional force does not cause variabilities on the borderline curve, so in this crossing region, in which the borderline variability would cause more threshold variabilities, this condition would present little uncertainties around the stability threshold.

Figure 10 presents the system with a 150 N additional load on the bearing, also being the only parameter presenting variability, which was of the standard deviation of 5% of the mean value. It is observable that the change on the curves crossing region generates more uncertainties around the stability threshold.

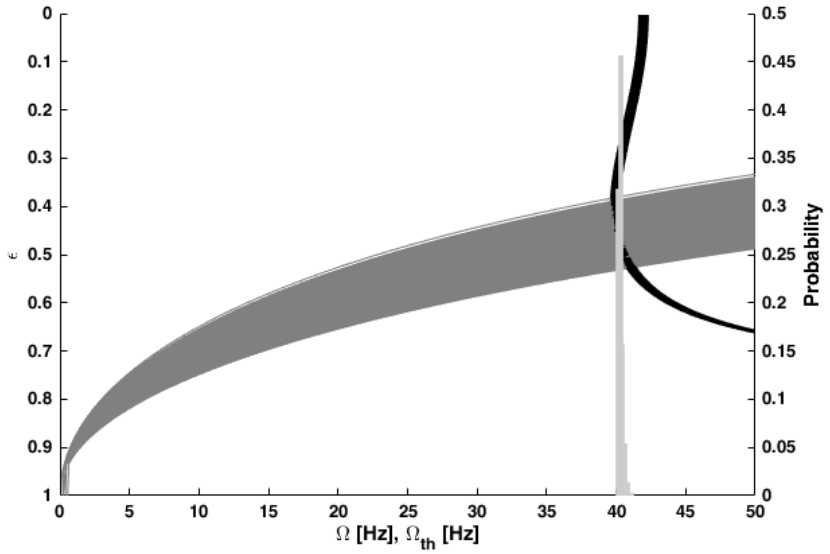

Figure 8. Startup curves (gray), borderline curves (black) and histogram of the stability threshold (light gray vertical bars) for the considered system with an 2.5kg disc mass and 80 N of additional load. Variabilities on the oil viscosity and bearing clearance

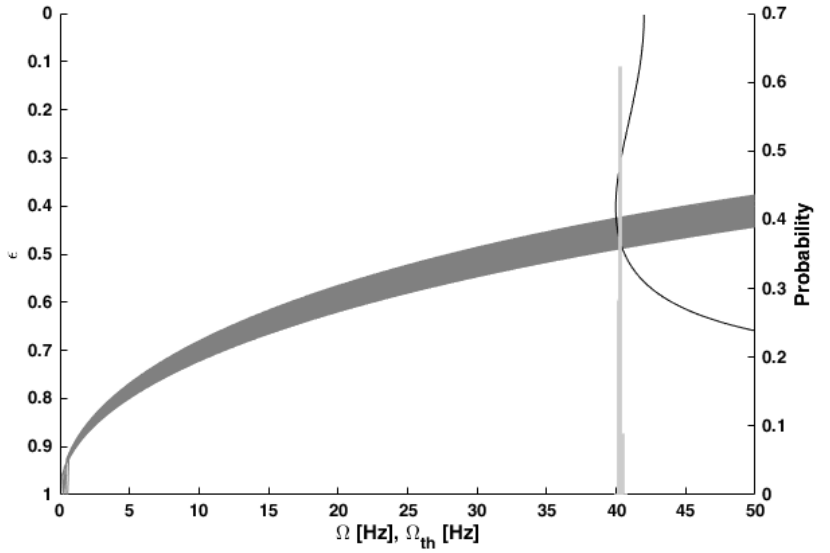

Figure 9. Startup curves (gray), borderline curves (black) and histogram of the stability threshold (light gray vertical bars) for the considered system with an 2.5kg disc mass and 80 N of additional load. Variability on the additional load

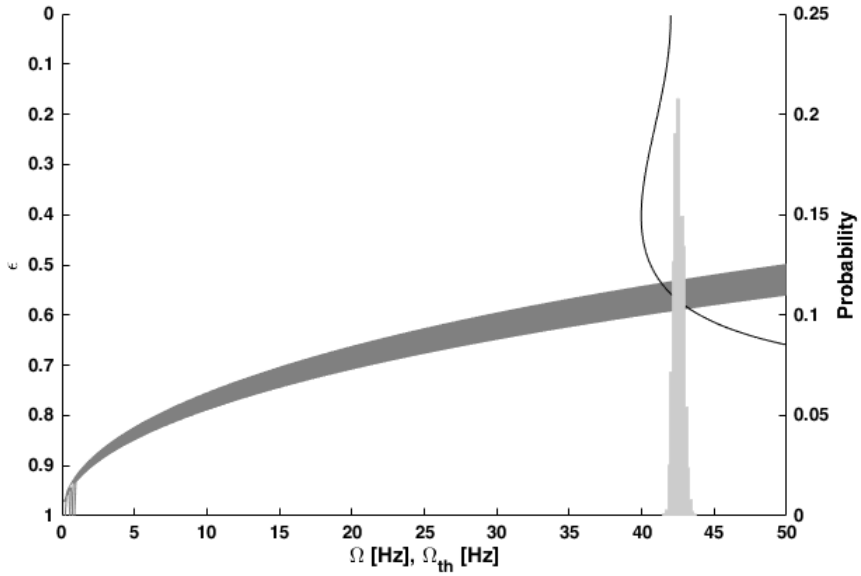

Figure 10. Startup curves (gray), borderline curves (black) and histogram of the stability threshold (light gray vertical bars) for the considered system with an 2.5kg disc mass and 150 N of additional load. Variability on the additional load

5. CONCLUSION

This paper intends to analyze the influence of variabilities on bearing parameters and additional static force on the stability threshold of a Laval rotor with hydrodynamic bearings. Both rotor and hydrodynamic bearings represented by simple models, due to the high computational cost of the Monte Carlo Method. The Laval model, which represents the rotor, is suitable for the purpose of this analysis, as well as the stiffness and damping coefficients of the bearings obtained by the consideration of linear forces. Also, the models were the same as the previous considered study of Visnadi and Castro (2018), which is important for comparisons made.

The parameters presenting variations were the bearing clearance and the oil viscosity. The bearing clearance may vary due to wear and the oil viscosity may vary due to temperature variations. These parameters were modeled by a Gamma distribution and had a 5% of coefficient of variance (ratio between the variance and the mean value).

The number of objects in the sample for the Monte Carlo simulations were 5,000, determined by a convergence analysis comparing histograms of the results. The same disc masses of the previous study of Visnadi and Castro (2018) were considered and the same observations about the stability threshold were made.

The maximum safe rotational speed decreases as the mass increases and the length of the instability zone depends on how the borderline curve behaves on the crossing zone with the startup curve. When considering a system with additional load, the natural frequency isn't modified, so that the maximum rotational speed tends to increase with an increase of the additional load. Variabilities of this additional load don't cause variabilities on the borderline curve, so it only will cause considerable variabilities if the startup curves crosses the borderline curve on the region in which it is approximately constant on the bearing eccentricity ratio with any rotational speed.

This study confirms that, the higher the static load on the bearing, the higher are the uncertainties about the stability threshold. A previous study (Visnadi and Castro, 2018) noted that by changing the disc mass of the rotor, but it also changes the natural frequency of the system, which may not represent real cases. This study showed that this increase of uncertainties also occurs when the static load is increased independently of the disc mass, which is more likely to occur on a real system. So, it confirms that considering uncertainties is important for determining the maximum safe operational speed of rotors supported by hydrodynamic bearings, especially when they are heavy-loaded.

6. ACKNOWLEDGEMENTS

The authors would like to thank Fapesp Grant #2015/20363 and Petrobras Brazil for the financial support to this research and LAMAR Unicamp.

7. REFERENCES

Devroye, L., 1986, Non-uniform Random Variate Generation. Springer-Verlag, New York /Berlin/Heidelberg/Tokyo.

Jaynes E, 1957a, “Information theory and statistical mechanics”. *Phys Rev* 106(4):1620–1630

Jaynes E, 1957b, “Information theory and statistical mechanics II.” *Phys Rev* 108(2):171–190

Krämer, E.,1993, *Dynamics of Rotors and Foundations*. Springer-Verlag, Berlin.

Lund, J. W., 1987, “Review of the Concept of Dynamic Coefficients for Fluid Film Journal Bearings”. Transactions of the ASME – Journal of Tribology. Vol. 109, p.37-41.

Montgomery, D. C., Runger, G. C., 2014, *Applied Statistics and Probability for Engineers*, John Wiley & Sons, New York.

Newkirk, B, L., Taylor, H. D. Shaft whipping due to oil action in journal bearings. General Electric Review, v.28, n. 8, 1925.

Ocvirk, E. W., 1952, “Short bearing approximation for full journal bearings”, *National Advisory Committee for Aeronautics*, Technical Note 2808, Cornell University (USA).

Reynolds, O., 1886, “On the Theory of Lubrication and its Application to Mr. Beauchamp Tower’s Experiments Including an Experimental Determination of the Viscosity of the Olive Oil”. *Phios. Trans. R. Soc. London*, Series A, 177(1), 157-234.

Shannon, C. E., 1948, “A mathematical theory of communication”. *Bell System Technical Journal*, 27, 379-423 and 623-659.

Visnadi, L., Castro, H. F. Uncertainty analysis on stability of a flexible rotor with lubricated bearings. Proceedings of the ICVRAM-ISUMA UNCERTAINTIES Congress. Brazil, Apr 2018.

8. RESPONSIBILITY NOTICE

The authors are the only responsible for the printed material included in this paper.